JOURNAL OF CHEMICAL & ENGINEERING DATA

ARTICLE

pubs.acs.org/jced

Thermodynamic Studies of a Nanowire-Shaped β-FeOOH Nanofluid Produced by a Solvothermal Route

Zhaodong Nan*,† and Zhicheng Tan‡

†College of Chemistry and Chemical Engineering, Yangzhou University, Yangzhou 225002, China

‡Thermochemistry Laboratory, Dalian Institute of Chemical Physics, Chinese Academy of Sciences, Dalian 116023, China

Supporting Information

ABSTRACT: An *n*-butanol-based nanofluid containing nanowire-shaped β-FeOOH was synthesized by a solvothermal method. The nanofluid was stable for 7 days without any precipitation with 3.0 mM SDBS as stabilizer. Uniform β-FeOOH nanowires with high aspect ratios were fabricated. The heat capacities of the obtained β-FeOOH sample, the base fluid, and the nanofluid were determined by an adiabatic calorimeter. Smoothed heat capacities and thermodynamic functions of the obtained samples, such as $H(T/\mathrm{K}) - H(298.15\ \mathrm{K})$ and $S(T/\mathrm{K}) - S(298.15\ \mathrm{K})$, were calculated based on the fitted polynomials and the relationships of the thermodynamic functions. These results are very useful to apply to the as-produced nanowire-shaped β-FeOOH and the nanofluid in engineering fields.

INTRODUCTION

Since the conception of nanofluids was proposed for the first time by Choi in 1995,[1] there has been intensive research interest not only for their important applications but also for their scientific and technological importance. It was reported that the thermal conductivity of these nanofluids was enhanced compared to the base fluids.[2−11] The reasons for the thermal conductivity enhancement in nanofluids have also been investigated.[12−14] In our previous report,[15] thermodynamic properties of a water-based hematite nanofluids were determined.

The polymorphs of iron oxyhydroxide consist of α-FeOOH (goethite), β-FeOOH (akaganeite), and γ-FeOOH (lepidocrocite).[16] Among these iron oxyhydroxides, β-FeOOH, as a stable iron oxide, which has a large tunnel-type structure, has received wide attention because of its unique properties. As a promising candidate for an electrode material, β-FeOOH exhibits good electrochemical properties with a high theoretical discharge capacity (302 $\mathrm{mA \cdot h \cdot g^{-1}}$).[17] β-FeOOH has been used as a precursor for the preparation of ferromagnetic α-Fe_2O_3.[18,19] In our previous paper,[20] thermodynamic properties of rod- and spindle-shaped β-FeOOH crystals were studied. Over the past decades, one-dimensional (1D) nanostructured materials, such as nanotubes, nanorods, or nanowires, have attracted extensive attention, because these materials have unique electronic, optical, chemical, and thermal properties and widespread potential applications in optics, electronics, magnetics, catalysis, sensors, biotechnology, and even as building blocks for nanoscale devices.[21−28] Thermodynamic properties of carbon nanotubes have been studied in our laboratory.[29] However, to the best of our knowledge, the molar heat capacities of one-dimensional β-FeOOH have not been reported so far. It is of great significance to obtain the molar heat capacities of one-dimensional β-FeOOH and furthermore to fully understand this material.

Herein, stable *n*-butanol-based β-FeOOH nanofluids and β-FeOOH nanowires were prepared through a one-step solvothermal method. The heat capacities of the nanofluid, base fluid, and solid β-FeOOH nanowires were measured by a high-precision automatic adiabatic calorimeter. To our best knowledge, *n*-butanol-based nanofluids have not been investigated until now.

EXPERIMENTAL SECTION

All chemicals were of analytical grade and used without further purification. A typical experiment was as follows: 3.0 mmol of $FeCl_3 \cdot 6H_2O$ and 0.5 mmol of urea were mixed in 50 mL of *n*-butanol. An anionic surfactant, sodium dodecyl benzene sulfonate (SDBS), was added into the solution, in which the concentration of SDBS was controlled at 3.0 mM. The solution was heated to 70 °C and maintained for 5 h. The solution subsequently cooled down to room temperature naturally. The nanofluid was formed. The solid sample was obtained by centrifuging the nanofluid and washing several times with distilled water and alcohol, sequentially.

The crystalline phase of the as-prepared solid product was characterized by a Rigaku D/MAX-XA power X-ray diffraction meter with Cu Kα radiation (λ = 1.5405 Å). A scanning rate of 0.1 $\mathrm{deg \cdot s^{-1}}$ was applied to record the pattern in the 2θ range of (10 to 700) deg. The mean size and morphology of the solid product was examined by a transmission electron microscope (TEM, Hitachi, model H-800) using an accelerating voltage of 200 kV.

A high precision automatic adiabatic calorimeter was used to determine the heat capacities of the as-prepared nanofluids, base fluids, and solid hematite nanoparticles in the temperature range of (290 to 335) K. The calorimeter was established in the Thermochemistry Laboratory of the Dalian Institute of Chemical Physics, Chinese Academy of Sciences. The principle and

Special Issue: John M. Prausnitz Festschrift

Received: August 21, 2010
Accepted: November 1, 2010
Published: November 17, 2010

Figure 1. Photograph of the as-produced nanofluid deposited for 7 days.

structure of the adiabatic calorimeter have been described in detail elsewhere.[14,30] The temperature increment was controlled to be (2 to 3) K during the whole experimental process. The mass of the solid product used for the molar heat capacity measurement was 1.53875 g, which is equivalent to 0.017317 mol, based on the corresponding molar mass of 88.858 $g \cdot mol^{-1}$. The volume of the nanofluids and base fluids used for the heat capacity measurements was about 4.6 mL.

Before the determination of the heat capacity of the as-obtained samples, the reliability of the automatic adiabatic calorimeter was verified via measurements of the α-Al_2O_3 reference standard material. On the basis of our experimental results, the deviations were within ± 0.2 % compared with the values recommended by the National Bureau of Standards in the temperature range of (80 to 400) K.[31]

RESULTS AND DISCUSSION

After depositing for 7 days, the image of the as-obtained nanofluid is shown in Figure 1. No precipitate was found in the as-prepared nanofluid. This result shows that a stable *n*-butanol based nanofluid was obtained in the present conditions. Various concentrations of SDBS were added into the reaction system to study the effects of SDBS on the stability of the nanofluid, in which other experimental conditions were kept the same. The images of these nanofluids after depositing for 7 days are shown in the Supporting Information as Figure S1. Yellow precipitation was found at the bottoms of the test tubes shown in Figure S1 parts A, B, and C, in which the concentrations of SDBS were equal to (0, 1.0, and 2.0) mM, respectively. These results demonstrate that the nanofluid becomes more stable when the concentration of SDBS increased to 3.0 mM. Li et al. reported that the stability of a water-based Cu nanofluid was increased with increasing concentration of SDBS because the phenyl sulfonic group adsorbed on the copper particles.[32] In the present study, the phenyl sulfonic group may adsorb on the surface of the as-produced particles. These groups induced the net negative charge of the particles surface and also increased the repulsive forces among these particles.

The solid product was obtained by centrifuging the nanofluid. The crystal structure of the resulting sample was characterized by using the X-ray powder diffraction (XRD) technique. Figure 2 shows the typical XRD pattern of the sample. All reflection peaks can be readily indexed to a tetragonal β-FeOOH phase with lattice parameters $a = (10.53 \pm 0.01)$ Å and $c = (3.03 \pm 0.01)$ Å, which are in agreement with the standard file of β-FeOOH (JCPDS 34-1266). XRD patterns of the solid samples produced under various concentrations of SDBS are shown in the Supporting Information. No effect of concentration of SDBS on the structure of the solid sample was found.

The morphology of the as-synthesized solid product was investigated by TEM analysis. Figure 3 represents the typical TEM image of the as-prepared sample, where the sample with high yield (almost 100 %) wire-shaped morphology can be found. The diameter of the wire was determined to be about (3 to 5) nm, and the length was about (30 to 90) nm. The aspect ratio is about 6 to 30.

The experimental heat capacity of the as-prepared β-FeOOH nanowires was determined by a high-precision automatic adiabatic calorimeter in the temperature range (290 to 350) K. The curve of the experimental molar heat capacities of the β-FeOOH nanowires is shown in Figure 4 and listed in Table 1. To compare the heat capacities of various morphologies of β-FeOOH, the heat capacities of rod- and spindle-shaped β-FeOOH are shown in Figure 4. The result obtained from Figure 4 indicated that the heat capacity of the nanowire-like β-FeOOH is the highest throughout this temperature range. A similar result was obtained for hematite nanoparticles,[15] for which the molar heat capacity of a nanoparticle is always higher than the same normal particle. The surface area of the nanowire-like β-FeOOH is the highest among three kinds of β-FeOOH particles. This may result in an increase of the values of the heat capacity for nanoparticles.

The experimental molar heat capacities of the solid product were fitted to a polynomial equation with respect to reduced temperature (X) via a least-squares fitting.

$$C_{p,\mathrm{m}}/\mathrm{J \cdot K^{-1} \cdot mol^{-1}} = -1.0848X^3 + 1.277X^2 + 8.8191X + 92.12 \quad (1)$$

where the coefficient of determination R^2 is 0.9994, and the reduced temperature is calculated based on the equation $X = (T - 321.04)/21.42$. The smoothed molar heat capacities of the solid sample were calculated based on the fitted equation, and the results are listed in Table 2. The changes of the thermodynamic functions of the β-FeOOH nanowires, such as ΔH and ΔS, were also calculated by the following thermodynamic equations:

$$\Delta H = H(T/\mathrm{K}) - H(298.15) = \int_{298.15}^{T} C_{p,\mathrm{m}}\, \mathrm{d}T \quad (2)$$

dx.doi.org/10.1021/je1008679 |J. Chem. Eng. Data 2011, 56, 915–919

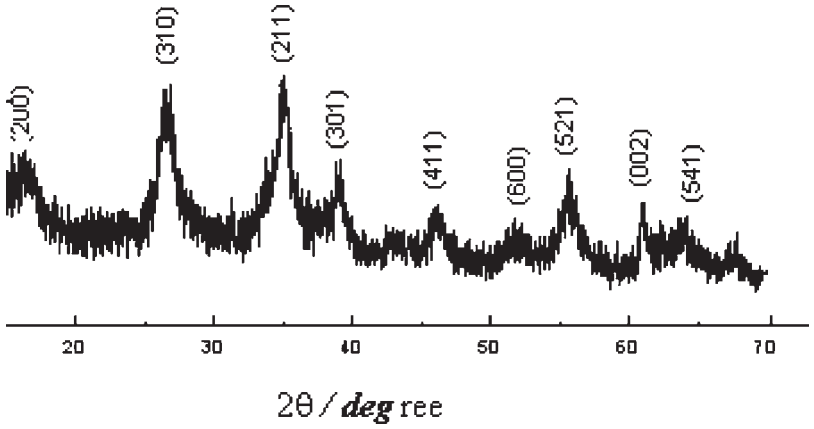

Figure 2. XRD patterns of the as-produced β-FeOOH particles.

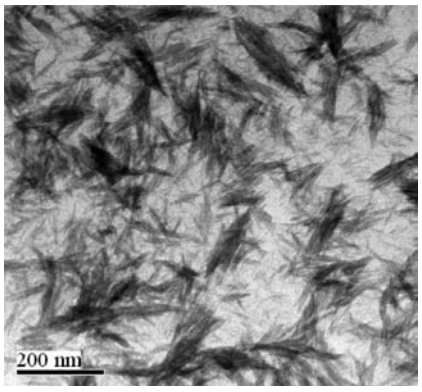

Figure 3. TEM image of the as-produced β-FeOOH nanowires.

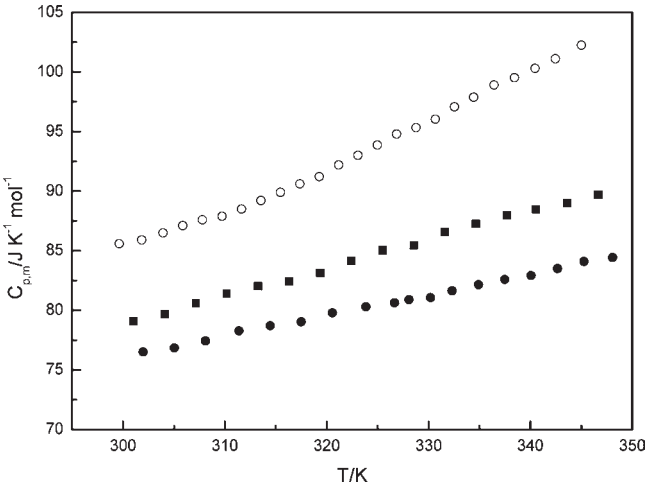

Figure 4. Curves of molar heat capacity of various morphologies of β-FeOOH nanowires vs thermodynamic temperature. ○, nanowire; ●, rod; ■, spindle.

$$\Delta S = S(T/\mathrm{K}) - S(298.15) = \int_{298.15}^{T} \frac{C_{p,\mathrm{m}}}{T}\,\mathrm{d}T \qquad (3)$$

The calculated changes in the thermodynamic functions of the β-FeOOH nanowires, which were the values of the enthalpy and entropy of the samples relative to the reference temperature 298.15 K, are also given in Table 2 at 5 K intervals. According to Table 2, it is shown that the value of ΔS increased as the

Table 1. Molar Heat Capacity of the As-Prepared Wire-Shaped β-FeOOH

T	$C_{p,\mathrm{m}}$	T	$C_{p,\mathrm{m}}$
K	$J\cdot K^{-1}\cdot mol^{-1}$	K	$J\cdot K^{-1}\cdot mol^{-1}$
299.62	85.602	323.07	93.005
301.83	85.899	324.97	93.873
303.92	86.496	326.87	94.800
305.86	87.103	328.76	95.331
307.79	87.592	330.65	96.028
309.72	87.887	332.54	97.077
311.64	88.496	334.42	97.883
313.55	89.211	336.43	98.899
315.46	89.904	338.44	99.516
317.37	90.602	340.45	100.30
319.27	91.221	342.45	101.10
321.17	92.206	345.01	102.24

Table 2. Thermodynamic Properties of the As-Prepared Wire-Shaped β-FeOOH

T	$C_{p,\mathrm{m}}$	ΔH	ΔS
K	$J\cdot K^{-1}\cdot mol^{-1}$	$J\cdot K^{-1}\cdot mol^{-1}$	$J\cdot K^{-1}\cdot mol^{-1}$
290	85.32	−2.850	−9.691
295	85.24	−1.123	−3.787
300	85.72	0.673	2.250
305	86.69	2.543	8.430
310	88.06	4.491	14.77
315	89.76	6.521	21.26
320	91.69	8.639	27.93
325	93.79	10.85	34.78
330	95.95	13.15	41.80
335	98.11	15.54	49.00
340	100.2	18.04	56.39
345	102.1	20.63	63.97
350	103.7	23.32	71.72
298.15	85.48	0	0

dx.doi.org/10.1021/je1008679 |J. Chem. Eng. Data 2011, 56, 915–919

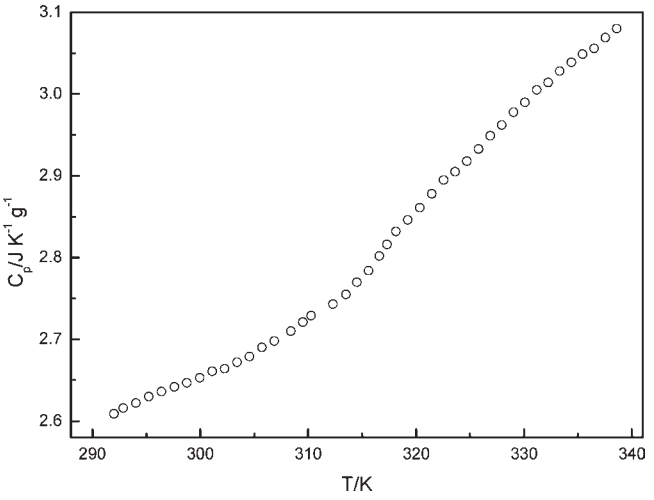

Figure 5. Curve of specific heat capacity of the nanofluid vs temperature.

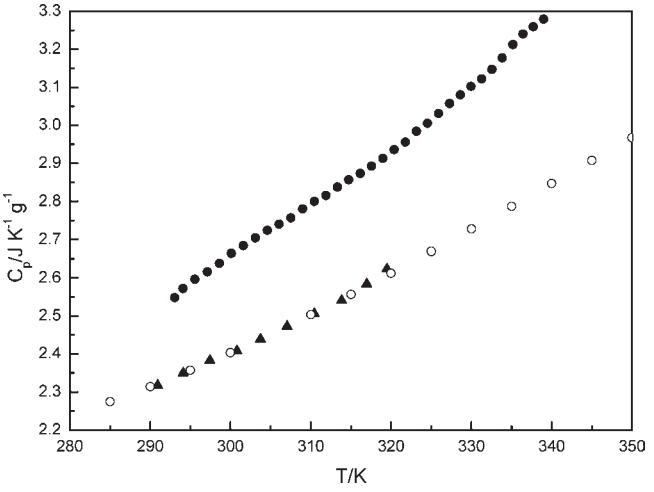

Figure 6. Curve of specific heat capacities vs temperature: ●, the base fluid; solid left-pointing triangle[34] and ○[35], *n*-butanol.

experimental temperature increased. These results demonstrate that the molecules of the sample became more active with increasing experimental temperature.

The specific heat capacities of the nanofluid and the base fluid were also determined by the adiabatic calorimeter and displayed in Figures 5 and 6, respectively. The base fluid was obtained by the removal of the solid nanoparticles from the nanofluid. As shown in Figures 4, 5, and 6, it is evident that the experimental heat capacities of the solid β-FeOOH nanowires, the nanofluid, and the base fluid are increased with increasing experimental temperature. To compare the specific heat capacities of the base fluid and pure *n*-butanol, the specific heat capacity of the *n*-butanol is also shown in Figure 6. The observed results from Figure 6 demonstrate that the specific heat capacity of the base fluid is higher than that of pure *n*-butanol. The heat capacity of a base fluid is always replaced by the pure solvent in experimental models for the calculation of the thermal conductivity coefficient of the nanofluid.[33] When the specific heat capacity of the base fluid was replaced by that of pure *n*-butanol, a deviation may be introduced into these models. Thus, it is necessary to determine the heat capacity of base fluid to calculate a thermal conductivity coefficient of a nanofluid.

CONCLUSIONS

An *n*-butanol-based nanofluid containing nanowire-shaped β-FeOOH was synthesized by a solvothermal method. Uniform β-FeOOH nanowires with high aspect ratios were fabricated. The diameter of the as-obtained nanowire-shaped β-FeOOH was about (3 to 5) nm, the length was about (30 to 90) nm. The heat capacities of the obtained β-FeOOH nanowire, the base fluid, and the nanofluid were determined by an adiabatic calorimeter. The heat capacity of the nanowire-like β-FeOOH is the highest among various morphologies of β-FeOOH particles. A polynomial equation of molar heat capacity of the as-prepared wire-shaped β-FeOOH with respect to reduced temperature (X) was established via a least-squares fitting. The heat capacity of the base fluid is greater than that of pure *n*-butanol. The thermodynamic functions, such as ΔH and ΔS, were also calculated.

ASSOCIATED CONTENT

Supporting Information. Photos of the as-prepared nanofluids and XRD patterns of the solid particles in Figures S1 and S2. This material is available free of charge via the Internet at http://pubs.acs.org.

AUTHOR INFORMATION

Corresponding Author

*Tel.: +86-514-87959896. Fax: +86-514-87959896. E-mail: zdnan@yzu.edu.cn.

Funding Sources

The authors gratefully acknowledge the financial support from the National Nature Science Foundation of China (No. 20753002) and the Natural & Scientific Grant of Jiangsu Province (BK2009181), China.

REFERENCES

(1) Choi, S. U. S. Enhancing Thermal Conductivity of Fluid with Nanoparticles. *ASME Pap.* **1995**, *231*, 99–105.

(2) Zhu, H. T.; Zhang, C. Y.; Tang, Y. M.; Wang, J. X.; Ren, B.; Yin, Y. S. Preparation of Carbon Nanotube-supported Palladium Nanoparticles by Self-regulated Reduction of Surfactant. *Carbon* **2007**, *45*, 203–206.

(3) Eastman, J. A.; Choi, S. U. S.; Li, S.; Yu, W.; Thompson, L. J. Anomalously Increased Effective Thermal Conductivities of Ethylene Glycol-based Nanofluids Containing Copper Nanoparticles. *Appl. Phys. Lett.* **2001**, *78*, 718–720.

(4) Jang, S. P.; Choi, S. U. S. Role of Brownian Motion in the Enhanced Thermal Conductivity of Nanofluids. *Appl. Phys. Lett.* **2004**, *84*, 4316–4318.

(5) Xue, Q.; Xu, W. M. A Model of Thermal Conductivity of Nanofluids with Interfacial Shells. *Mater. Chem. Phys.* **2005**, *90*, 298–301.

(6) Li, X. F.; Zhu, D. S.; Wang, X. J.; Wang, N.; Gao, J. W.; Li, H. Thermal Conductivity Enhancement Dependent pH and Chemical Surfactant for Cu-H_2O Nanofluids. *Thermochim. Acta* **2008**, *469*, 98–103.

(7) Xuan, Y.; Li, Q. Heat Transfer Enhancement of Nanofluids. *Int. J. Heat Fluid Flow* **2000**, *21*, 58–64.

(8) Zhu, H. T.; Lin, Y. S.; Yin, Y. S. A Novel One-step Chemical Method for Preparation of Copper Nanofluids. *J. Colloid Interface Sci.* **2004**, *277*, 100–103.

(9) Zhu, H. T.; Zhang, C. Y.; Tang, Y. M.; Wang, J. X. Novel Synthesis and Thermal Conductivity of CuO Nanofluid. *J. Phys. Chem. C* **2007**, *111*, 1646–1650.

(10) Lee, S.; Choi, S. U. S.; Li, S.; Eastman, J. A. Measuring Thermal Conductivity of Fluids Containing Oxide Nanoparticles. *ASME J. Heat Transfer* **1999**, *121*, 280–289.

(11) Kumar, D. H.; Patel, H. E.; Kumar, V. R. R.; Sundararajan, T.; Pradeep, T.; Das, S. K. Model for Heat Conduction in Nanofluids. *Phys. Rev. Lett.* **2004**, *93*, 144301–144304.

(12) Vadasz, P. Heat Conduction in Nanofluid Suspensions. *J. Heat Transfer* **2006**, *128*, 465–477.

(13) Keblinski, P.; Phillpot, S. R.; Choi, S. U. S.; Eastman, J. A. Mechanisms of Heat Flow in Suspensions of Nano-sized Particles (Nanofluids). *Int. J. Heat Mass Transfer* **2002**, *45*, 855–863.

(14) Tan, Z. C.; Sun, L. X.; Meng, S. H.; Li, L.; Zhang, J. B. Heat Capacities and Thermodynamic Functions of *P*-chlorobenzoic Acid. *J. Chem. Thermodyn.* **2002**, *34*, 1417–1429.

(15) Wei, C.; Nan, Z.; Wang, X.; Tan, Z. Investigation on Thermodynamic Properties of a Water-Based Hematite Nanofluid. *J. Chem. Eng. Data* **2010**, *55*, 2524–2528.

(16) Flynn, C. M., Jr. Hydrolysis of Inorganic Iron (III) Salts. *Chem. Rev.* **1984**, *84*, 31–41.

(17) Wang, X.; Chen, X. Y.; Gao, L. S.; Zheng, H. G.; Ji, M. R.; Tang, C. M.; Shen, T.; Zhang, Z. D. Synthesis of β-FeOOH and α-Fe_2O_3 nanorods and electrochemical properties of β-FeOOH. *J. Mater. Chem.* **2004**, *14*, 905–907.

(18) Sugimoto, T.; Muramatsu, A. Formation Mechanism of Monodispersed α-Fe_2O_3 Particles in Dilute $FeCl_3$ Solutions. *J. Colloid Interface Sci.* **1996**, *184*, 626–638.

(19) Mazeina, L.; Deore, S.; Navrotsky, A. Energetics of Bulk and Nano-Akaganeite, β-FeOOH: Enthalpy of Formation, Surface Enthalpy, and Enthalpy of Water Adsorption. *Chem. Mater.* **2006**, *18*, 1830–1838.

(20) Wei, C.; Wang, X.; Nan, Z.; Tan, Z. Thermodynamic Studies of Rod- and Spindle-shaped β-FeOOH Crystals. *J. Chem. Eng. Data* **2010**, *55*, 366–369.

(21) Alivisatos, A. Semiconductor Clusters, Nanocrystals, and Quantum Dots. *Science* **1996**, *271*, 933–937.

(22) Xia, Y.; Yang, P.; Sun, Y.; Wu, Y.; Mayers, B.; Gates, B.; Yin, Y.; Kim, F.; Yan, Y. One-Dimensional Nanostructures: Synthesis, Characterization, and Applications. *Adv. Mater.* **2003**, *15*, 353–389.

(23) Li, Z.; Lai, X.; Wang, H.; Mao, D.; Xing, C.; Wang, D. Direct hydrothermal synthesis of single-crystalline hematite nanorods assisted by 1,2-propanediamine. *Nanotechnology* **2009**, *20*, 245603.

(24) Sun, J.; Tang, Q.; Lu, A.; Jiang, X.; Wan, Q. Individual SnO_2 nanowire transistors fabricated by the gold microwire mask method. *Nanotechnology* **2009**, *20*, 255202.

(25) Huang, M.; Mao, S.; Feick, H.; Yan, H.; Wu, Y.; Kind, H.; Weber, E.; Russo, R.; Yang, P. Room-Temperature Ultraviolet Nanowire Nanolasers. *Science* **2001**, *292*, 1879–1899.

(26) Wang, Y.; Yang, H. Synthesis of iron oxide nanorods and nanocubes in an imidazolium ionic liquid. *Chem. Eng. J.* **2009**, *147*, 71–78.

(27) Cui, Y.; Lieber, C. Functional Nanoscale Electronic Devices Assembled Using Silicon Nanowire Building Blocks. *Science* **2001**, *291*, 851–853.

(28) Duan, X. F.; Huang, Y.; Cui, Y.; Wang, J. F.; Lieber, C. M. Indium phosphide nanowires as building blocks for nanoscale electronicand optoelectronic devices. *Nature* **2001**, *409*, 66–69.

(29) Nan, Z.; Wei, C.; Yang, Q.; Tan, Z. C. Thermodynamic Properties of Carbon Nanotubes. *J. Chem. Eng. Data* **2009**, *54*, 1367–1370.

(30) Tan, Z. C.; Sun, G. Y.; Sun, Y.; Yin, A. X.; Wang, W. B.; Ye, J. C.; Zhou, L. X. An adiabatic low-temperature calorimeter for heat capacity measurement of small samples. *J. Therm. Anal.* **1995**, *45*, 59–67.

(31) Ditmars, D. A.; Ishihara, S.; Chang, S. S.; Bernstein, G.; West, E. D. Enthalpy and heat-capacity standard reference material: synthetic sapphire (α-Al_2O_3) from 10 to 2250 K. *J. Res. Natl. Bur. Stand.* **1982**, *87*, 159–163.

(32) Li, X.; Zhu, D.; Wang, X. Evaluation on dispersion behavior of the aqueous copper nano-suspensions. *J. Colloid Interface Sci.* **2007**, *310*, 456–463.

(33) Zhou, S. Q.; Ni, R. Measurement of the Specific Heat capacity of Water-based Al_2O_3 Nanofluid. *Appl. Phys. Lett.* **2008**, *92*, No. 093123.

(34) Nan, Z.; Tan, Z. C. Thermodynamic Properties of the Binary Mixture of Water and *n*-Butanol. *J. Therm. Anal. Calorim.* **2007**, *87*, 539–544.

(35) Zorebski, E.; Chorazewski, M.; Traczyk, M. Excess Molar Heat Capacities for (1-Butanol + 1, 3-Butanediol) at Temperatures from (285 to 353) K. *J. Chem. Thermodyn.* **2005**, *37*, 281–287.